PARAMETERISATION OF THE AEROSOL INDIRECT CLIMATIC EFFECT

PACE

EVK2-CT-1999-00054

REPORT ON THE

FIRST PACE MEETING

P1: Jean-Louis Brenguier: Météo-France (F)
Co-ordinator

P2: Lothar Schüller: Freie Univ. Berlin (D)

P3: Hanna Pawlowska: Univ. of Warsaw (PL)

P4: Dave Roberts: The Met. Office (UK)

P5: Johann Feichter: Max Planck Institut (D)

P6: Jefferson Snider: Univ. of Wyoming (USA)

P7: Ulrike Lohmann: Dalhousie Univ. (CA)

P8: Surabi Menon: Columbia University (USA)

P9: Steve Ghan: Batelle Memorial Institute (USA)

15 Mai 2000

1. Introduction

The first PACE meeting was held from Mai 1 to 5 at the NASA Goddard Institute for Space Studies (NASA GISS/University of Columbia). The first two days were dedicated to the preparation of the workshop by the experimentalists of the project (Partners 1, 2, and 3). During the next two days experimentalists and modellers presented their contributions. The last day was devoted to the general discussion. The agenda of the meeting is reported in Appendix I.

2. Preparatory Meeting (1-2 Mai)

2.1 Participants

P1: J. L. Brenguier, S. Guibert, F. Troude
P2: L. Schüller, M. Schröder
P3: H. Pawlowska, S. Malinowski
P4: D. Roberts (Mai 2, only)
P8: S. Menon

2.2 Objectives

Present and discuss the latest results of the data analysis, evaluate how they fit the needs of the modellers, and structure the presentations for the plenary sessions.

2.3 Report

The first presentation was made by H. Pawlowska, who was in charge of the in situ data processing and interpretation during ACE-2. Followed a presentation by S. Malinowski, head of the Atmospheric Division at the Warsaw University Institute of Geophysics (IGUW Partner 3). S. Malinowski summarized recent developments at IGUW, on laboratory studies of the mixing processes at the micro-scale and 3-D LES modelling of boundary layer clouds.

In the afternoon, S. Menon gave an overview of the GISS general circulation model (GCM), with emphasis on the parameterisations of the aerosol/microphysics interaction, sub-grid cloud scheme, and radiative transfer.

The second day meeting started with a review of slides taken from the Merlin-IV during the experiment, showing various examples of the sampled clouds. This was followed by a presentation of the closure exercise on aerosol/cloud microphysics by S. Guibert. After a general discussion on the structure of the plenary sessions, the meeting was deferred early in the afternoon to allow for individual preparation.

3. Plenary Sessions Meeting (3-5 Mai)

3.1 Participants

P1: J. L. Brenguier, S. Guibert, F. Troude
P2: L. Schüller, M. Schröder
P3: H. Pawlowska, S. Malinowski
P4: D. Roberts, A. Jones
P5: J. Feichter
P6: J. Snider
P7: U. Lohmann
P8: S. Menon, A. Del Genio
P9: S. Ghan

3.2 Objectives

- For the experimentalists to provide an overview of the experiment and of the available data, their accuracy and statistical significance; to describe the data processing and their interpretation in term of physical processes; to summarize the present results of the closure experiments and the possible improvements.
- For the modellers to describe the parameterisations that are used in their GCM for the physical processes involved in the aerosol indirect effect (AIE), with emphasis on the physical significance of the model variables.

3.3 Data Analysis and Model Parameterisations

After a welcome speech by S. Menon, J. L. Brenguier made a short introduction on the PACE project and the aims of the meeting. The first year of the project is dedicated to tasks 1 and 2, that are related respectively to the physical processes involved in the AIE and the most suited physical variables for their description. In practical terms, this meeting aims at identifying the actions that shall now be taken within the next 6 months for allowing initialisation of the single column models (SCM) and their validation.

3.3.1 Aerosol/Cloud Microphysics Interaction

3.3.1.1 Model Parameterisations

P4: Hadley Centre (A. Jones):

CDNC is diagnosed from the number concentrations of the non-sea-salt sulphate and sea-salt aerosols, as:

$N_d = \max[\,375\,(1-\exp^{-0.0023A}), N_{\min}\,]$

where $A=A_{SO4}+A_{SS}$ is the number concentration of the hygroscopic aerosols. *SO4* and *SS* refers to sulphate and sea-salt respectively. $N_{min} = 5\ cm^{-3}$ over the ocean and land ice-sheets, and $N_{min} = 35\ cm^{-3}$ over land. The sulphate number concentration is derived from the sulphate mass by assuming a log-normal distribution with $r_m=0.05\ \mu m$ and $s=2$. The sea-salt number concentration is a function of the wind speed at the ocean surface. It follows an exponential decay with height with a scale height of *900 m.*

This parameterisation is empirically based and it does not consider the effect of vertical velocity on the number of activated nuclei.

P8: GISS (S. Menon):

CDNC is diagnosed from the mass concentrations of non-sea-salt sulphate (S), sea-salt (SS), and organic matter (OM), as:

$$\text{Log}\,(N_d) = 2.25 + 0.63 \times \text{Log}(S) + 0.01 \times \text{Log}(OM), \text{ over the ocean,}$$

$$\text{Log}\,(N_d) = 2.25 + 0.63 \times \text{Log}(S) + 0.01 \times \text{Log}(OM) + 0.16 \times \text{Log}(SS), \text{ over land.}$$

These parameterisations are based on the data from Tenerife by Borys et al. 1998 and from Putaud et al. 2000.

CDNC is also diagnosed from aerosol number concentration (Gultepe and Isaac, 1999) as follows:

$$N_d = 162 \log (N_{acS} + N_{acOM} + N_{acSS}) - 273, \text{ over the ocean}$$

$$N_d = 298 \log (N_{acS} + N_{acOM}) - 595 \text{ over land.}$$

where N_{acS}, N_{acOM} and N_{acSS} are the aerosol concentrations within cloud for sulphate, organic matter and sea-salt and are obtained empirically from data over North-eastern America (Leaitch et al. 1992, Liu et al. 1996, Lohmann et al. 2000-a). For sea-salt, aerosol concentration is obtained as a function of size and is given as:

$$N_{acSS} = 3\ (\text{mass of SS})/(4\ \pi\ r^3\ \rho_{ss})$$

Both these parameterisations for CDNC are empirically based and do not explicitly consider the effect of vertical velocity on the number of activated nuclei. Cloud turbulence (the cloud top entrainment factor, a diagnostic in the GISS GCM, is used as a proxy for cloud turbulence.) is used as a tuning factor to enhance the CDNC at high values of turbulence or suppress CDNC for low turbulence.

P9: PNNL (S. Ghan):

In this model CDNC is treated as a prognostic variable (Ghan et al., 1997). The nucleation rate $R_{nucl\text{-}N}$ is represented in terms of the number nucleated for a new cloud

$$R_{nucl-N} = \frac{1}{\Delta t}\int_0^\infty N_n(w)p(w)dw\ ,$$

or in terms of the convergence of a droplet nucleation flux at the base of an existing cloud,

$$R_{nucl-N} = \frac{1}{\Delta z}\int_0^\infty w_b N_n(w)p(w)dw\ .$$

The number nucleated is parameterised from Köhler theory as an analytic function of the updraft velocity w and the number concentration N_i, geometric standard deviation σ_i, number mode radius a_{mi} and bulk hygroscopicity B_i of an arbitrary number of log-normal aerosol modes (Abdul-Razzak and Ghan, 2000),

$$N_n(w) = \sum_{i=1}^{I} N_i \frac{1}{2}\left[1 - erf(u_i)\right]$$

where I is the number of aerosol species, $u_i = \frac{2\ln(S_{mi}/S_{max})}{3\sqrt{2}\ln s_i}$, and S_{max} is the maximum supersaturation of the updraft,

$$S_{max}^2 = 1/\sum_{i=1}^{I} \frac{1}{S_{mi}^2}\left[f_i\left(\frac{V}{h_i}\right)^{3/2} + g_i\left(\frac{S_{mi}^2}{h_i + 3V}\right)^{3/4} \right]$$

$$f_i = 0.5\exp(2.5\ln^2 s_i), \quad g_i = 1 + 0.25\ln s_i$$

$$S_{mi}^2 = \frac{4}{B_i}\left(\frac{A}{3a_{mi}}\right)^3, \quad V = \frac{2A}{3}\left(\frac{aw}{G}\right)^{1/2}, \quad h_i = \frac{(aw/G)^{3/2}}{2\pi r_w g N_i},$$

where A is the surface tension of water, ρ_w is the density of water, and G, a and g are thermodynamic coefficients. The bulk hygroscopicity is determined from the volume-weighted average of the hygroscopicity of each component (non-sea-salt sulphate, sea-salt, organic carbon, black carbon, and dust) of the mode (Aitken, accumulation, or coarse). The probability distribution of vertical velocity $p(w)$ is represented as a Gaussian distribution with the mean from the mean grid vertical velocity $\overline{w}$ and the standard deviation diagnosed from the mean turbulent kinetic energy (TKE).

P7, Dalhousie Univ. (U. Lohmann):

The parameterisation is similar to the one described above for PNNL, with a modified nucleation (Lohmann et al. 1999), making use of observational data by Lin and Leaitch (1996). A maximum concentration of activated nuclei is derived as:

$$N_{max} = \frac{N_a \times 1.9w}{1.9 \times w + aN_a},$$

where $a = 0.023\ s^{-1}cm^4$. N_d is then calculated as:

$$N_d = 0.1 \times N_{max}^{1.27}$$

The same formula as above is used as a source term in the CDNC budget equation, and hence it is divided by the time step:

$$R_{nucl-N} = \frac{N_d}{\Delta t},$$

3.3.1.2 Closure Experiments

In the introduction, J. L. Brenguier made a brief description of the instrumental set-up during the ACE-2 Cloudy-Column experiment, with a detailed list of the instruments mounted on the various aircraft and he presented the summary of the field campaign (Brenguier et al. 2000-b).

H. Pawlowska then described the procedure that was designed for the calculation of the CDNC characteristic value. It represents the mean value of the CDNC frequency distribution after selection of samples that are not affected by mixing with the overlying dry air nor by drizzle scavenging. This value is regarded as directly representative of the activation process on the background aerosol and it is used as a reference for each case study. It varies from 50 cm^{-3} for the most marine case (June 25) to 244 cm^{-3} for the most polluted one (July 9). For each case the frequency distribution of the measured CDNC values, after selection, is distributed between 0.5 and 1.5 of the mean value. Only 8 cases have been processed because the procedure makes use of the series of ascents and descents with the Merlin-IV, for a better statistical significance of the results. Such trajectories were not always performed, especially during the inter-calibration flights (Pawlowska and Brenguier, 2000-a).

A discussion of the closure experiments involving aerosol, CCN, and CDNC was led by J. Snider (Partner 6, Univ. of Wyoming), in collaboration with S. Guibert and J. L. Brenguier (Partner 1, Météo-France).

Sarah Guibert discussed the ways in which the aerosol data obtained from both the Merlin and the Punta del Hidalgo (PDH) ground station have been compared. For these analyses, both Köhler theory and Köhler theory

combined with a description of the droplet growth process were utilized. The former was used to predict particle size at specified values of relative humidity (*RH*), based on the aerosol composition measurements made at PDH. When combined with the PDH size spectrum, this result was used to infer the cumulative number of droplets activated at a specified supersaturation (i.e., the CCN activation spectrum). The combination of Köhler theory, plus droplet growth kinetics applied within the context of a parcel model, were used to model the time evolution of supersaturation. Also predicted was concentration of activated droplets. This prediction of CDNC was compared to the measured CDNC values. We refer to the processes described by Köhler theory and by the droplet activation process as the static and kinetic steps, respectively. A summary of S. Guibert's work is described below, details can be found in Guibert et al. (2000).

a- Dry (RH=20%) aerosol size distributions measured at PDH were compared to the ones measured on the Merlin-IV with the PCASP. Except for three cases (1, 19, and 21 July), the agreement is within the instrumental uncertainties. This result suggests that the PDH data set is representative of aerosol properties at the flight location.

b- Wet (RH=92 %) aerosol size distributions predicted from PDH measurements (static step) were compared to spectra measured on the Merlin-IV with the FSSP-300. The predicted concentrations cumulated within the overlap diameter range (0.3 to 1 µm) are systematically overestimated by a factor of about 2 to 10. This lack of closure, suggests that a large measurement bias exists in one of the three measurement systems (PDH or FSSP-300 size distribution or the Merlin measurement of relative humidity). The alternative explanation is a deficiency in the Köhler theory when applied to the complex mixtures of particles and chemical species that exist in the atmosphere. We note that Köhler theory has been validated for aerosols of known composition and mixing state.

c- CCN activation spectra predicted from the PDH measurements (static step) were compared to activation spectra measured on the Merlin-IV with the UWYO CCN chamber. The predicted concentrations of activated nuclei are consistent, within the UWYO CCN measurement uncertainties, for the marine cases. However, the prediction overestimates the activated concentration, for the polluted cases, especially at low supersaturations (S<0.4%). At larger values of supersaturation, and for all flights (polluted and unpolluted), the disparity is smaller and indicates a degree of closure that is consistent with the CCN measurement uncertainty (±50%). The disparity cannot be reconciled by a factor of two uncertainty in the aerosol soluble fraction.

d- CDNC values predicted by combining the static and kinetic steps, initialised with the PDH aerosol data and vertical velocity from the Merlin, were compared to measurements of CDNC from the Merlin-IV. In order to take into account the variability of the vertical velocity, the comparison was performed using probability density functions (PDF) of the measured variables (w and CDNC). The predicted values of CDNC were shown to be larger than the observations by a factor that ranged between 1.2 and 3.

J. Snider presented the results of a successful CDNC closure experiment. Here CDNC values predicted by combining the static and kinetic steps, initialised with the UWYO CCN data and vertical velocity from the Merlin-IV, were compared to the measurements of CDNC from the Merlin-IV. As in (d) above, the measured PDF of vertical velocity is converted into a PDF of CDNC that is then compared to the measured PDF(CDNC). The agreement between the two distributions is within the uncertainty of the measurements.

To conclude the closure exercise, S. Guibert presented a comparison of the observed N_{mean} values for each case with the values diagnosed using the GCM parameterisations of the PACE partners, initialised with the PDH measurements of aerosol properties. Table I summarizes the exercise for 8 flights of the ACE-2 project, classified as clean and polluted. The comparison with the CDNC values measured in situ, in Fig. 1 for the clean cases and Fig. 2 for the polluted ones, shows that predictions of CDNC are generally overestimated, especially for the polluted cases. Further, the most physically based parameterisations of partners 7 and 9 were associated with larger overestimation. This result is the first attempt to compare GCM parameterisations with the ACE-2 data set and hence shall be considered as preliminary. In particular, the comparison cannot be considered as significant as long as there is a bias between the measured CDNC values and those derived using the Köhler and parcel models initialised with the measured aerosol properties. The main effort in the analysis of the activation process will thus be to identify the origin of the bias in order to produce an aerosol data set that can be efficiently used for validation of the parameterisations.

Date	21/06/97	24/06/97	25/06/97	26/06/97	04/07/97
Flight number	#18	#19	#20	#21	#24
Flight letter	A	B	C	D	F
Air masse	intermediate	clean	clean	clean	intermediate
N_{mean}, cm^{-3}			**71**	**54**	
*** N_{mean}, cm^{-3}**	**62**	**45**	**43**	**60**	**77**
N_a, cm^{-3} (SO_4,SS,OC,BC,dust)	94	42	45	39	57
In cloud * $W_{95\%}$, $m.s^{-1}$	1.00	0.80	1.06	0.80	3.09
$N_{PDH\ mean}$, cm^{-3}	**189**	**105**	**109**	**79**	**174**
$N1_{mean}$, cm^{-3} (Lohmann/Ghan)	**169**	**78**	**78**	**72**	**208**
N2, cm^{-3} (Menon)	**112**	**48**	**52**	**56**	**68**
N3, cm^{-3} (Jones/Roberts)	**119**	**95**	**107**	**64**	**176**

Date	07/07/97	09/07/97	17/07/97	18/07/97	19/07/97	21/07/97
Flight number	#26	#30	#33	#34	#35	#36
Flight letter	G	H	I	J	K	L
Air masse	polluted	polluted	polluted	polluted	polluted	intermediate
N_{mean}, cm^{-3}		**245**	**111**	**179**	**130**	
*** N_{mean}, cm^{-3}**	**219**	**154**	**145**	**172**	**145**	**93**
N_a, cm^{-3} (SO_4,SS,BC,OC,dust)	408	228	147	239	261	108
In cloud * $W_{95\%}$, $m.s^{-1}$	0.80	0.81	0.80	0.80	0.60	1.60
$N_{PDH\ mean}$, cm^{-3}	**461**	**308**	**274**	**320**	**278**	**186**
$N1_{mean}$, cm^{-3} (Lohmann/Ghan)	**859**	**341**	**255**	**369**	**297**	**124**
N2, cm^{-3} (Menon)	**416**	**307**	**151**	**259**	**183**	**113**
N3, cm^{-3} (Roberts)	**352**	**255**	**194**	**263**	**275**	**155**

Table I : Comparison between the typical values of CDNC measured in situ (**N_{mean}**), the values predicted by the Köhler theory initialised with the PDH data (**N_{PDH}**), and the values calculated with the various parameterisations (N1, N2 and N3)

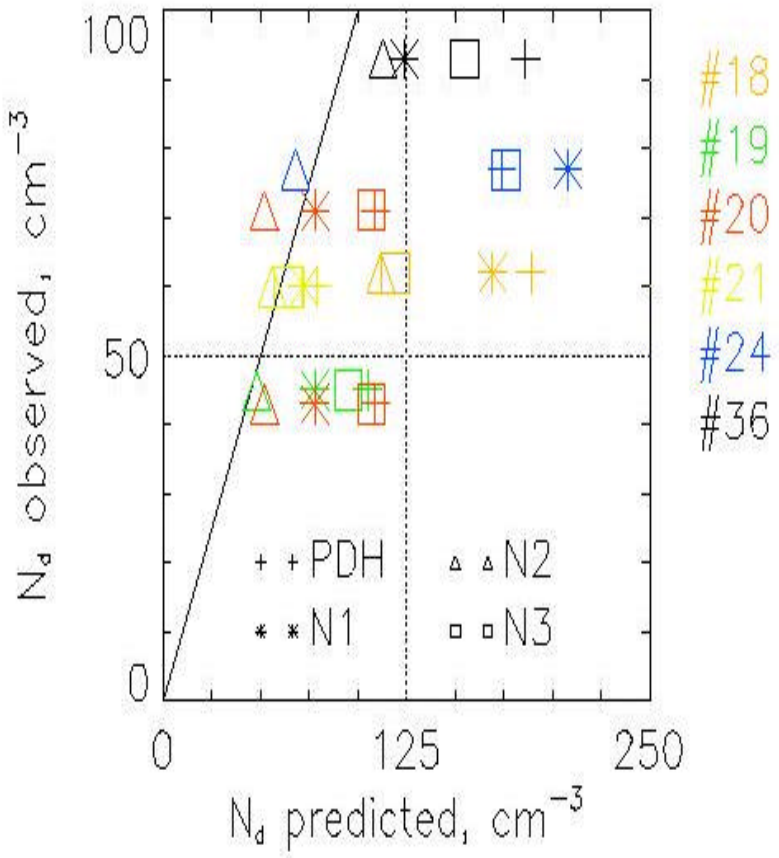

Figure 1: Comparison of the CDNC values of Table 1 for the clean cases

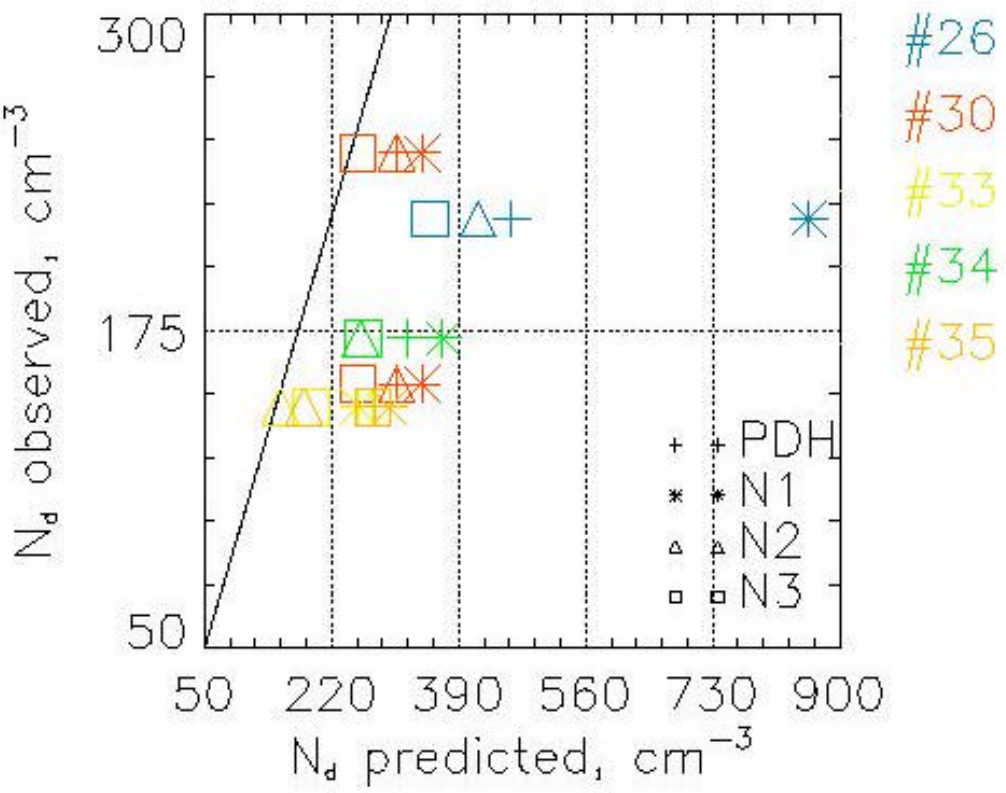

Figure 2: Comparison of the CDNC values of Table 1 for the polluted cases

3.3.2 Cloud/Radiation Interaction, Sub-Grid Cloud Fraction and Precipitation Efficiency

3.3.2.1 Model Parameterisations

All models that are used within the PACE project use the assumption of vertically homogeneous cloud layers. The radiative properties are parameterised in terms of optical thickness t and effective radius r_e. These two quantities are predicted from the liquid water content q_c or liquid water path W and the droplet number concentration N_d by the following relations:

$$t = \frac{3 q_c \cdot \Delta z}{2 \cdot r_e}$$

$$r_e^3 = \frac{3 q_c}{4p \cdot r_w \cdot kN} \quad \text{(Martin et al. 1994)}$$

where r_w is the density of water and k relates the volumne radius r_v to the effective radius r_e:

$$r_v^3 = k \cdot r_e^3 \,.$$

Different values of k are used depending on the character of the airmass (continental or maritime). The single scattering properties (extinction coefficient, single scattering albedo and asymetry factor resp. scattering phase function) as well as infrared emissivity, are calculated with Mie theory. The width of the droplet size distributions are kept constant.

The radiative transfer in several spectral bands is then computed with different codes, e.g. Edvards and Slingo (1996) for Hadley Centre or Rockel et. Al. (1991) for MPI.

P4: Hadley Centre (D. Roberts, A. Jones):

The radiative properties of liquid water cloud droplets are parameterised slightly differently in the Hadley Centre model, using a scheme developed from the one described by Slingo (1989). The extinction coefficient (per unit mass of liquid water) s_{ext}, single scatter albedo w and asymmetry parameter g are parameterised as functions of the droplet effective radius r_e as follows:

$$s_{ext} = A + B/r_e \quad , \qquad 1 - w = C + D r_e \quad , \qquad g = E + F r_e$$

The coefficients $A,...F$ are computed by fitting the results of "off-line" Mie theory calculations to these equations, averaging over the spectral bands to be used in the GCM. The total extinction due to the water in a cloudy layer in the model is then the product of s_{ext}, (with r_e determined by the Martin et al. 1994 formula) and the liquid water content in the grid box.

This model distinguishes between layer cloud amount (L) and convective cloud amount (C). The layer cloud amount is determined by the fraction of the triangular relative humidity distribution about the grid box mean value that exceeds $RH=100$ %. The width of the triangle is prescribed by setting a RH threshold. The convective cloud amount is determined by the mass of condensed water per unit area before precipitation. Together with the possibility of ice and water clouds, this scheme leads to four possible cloud types in a grid box: ice-layered, ice-convective, water-layered and water-convective, since ice and liquid water clouds are disjoint in the grid box. The properties of each cloud type are spatially uniform. Several overlap assumptions apply for the combination of clouds in different layers. For example, clouds in adjacent layers are arranged in such way, that they overlap maximally, i.e. producing the thickest possible cloud. This is not true, if clouds are separated by clear layers. In that case, clouds are arranged randomly. Convective and layer clouds overlap coherently when the layers are adjacent, but the ice and water portions overlap each other randomly even when the layers are adjacent.

Transmission and reflection coefficients are then computed for the four cloud types in each grid box. and the mean valued are calculated. The upward and downward directed radiative fluxes are then determined in the clear, the layer and the convective cloud portions of the grid box, using the overlap assumptions.

Cloud precipitation efficiency (second indirect effect) is based on the cloud scheme by Wilson and Ballard (1999), with water vapour + liquid water content and ice water content as prognostic variables. Among the various physical processes involved in the conversion scheme between these three variables, only the auto-conversion process is dependent upon CDNC. Three parameterisations have been tested:

$R_{AUTO} \propto q_c^{2.333} N_d^{-0.333}$	Tripoli and Cotton (1980)
$R_{AUTO} \propto q_c^{4.7} N_d^{-3.3}$	Beheng (1994)
$R_{AUTO} \propto q_c^{2.47} N_d^{-1.79}$	Khairoutdinov and Kogan (2000)

As might be expected, results differ widely depending on the parameterisation chosen.

Clouds also affect the distribution of aerosols in the model in various ways:

- Sites for aqueous phase oxidation of SO_2 to SO_4^{2-}.
- Rainout of dissolved SO_4^{2-} from clouds
- Turbulent deposition of dissolved SO_4^{2-}.

These processes consider cloud water in bulk. The only process which considers Nd specifically is the diffusive scavenging of Aitken-mode aerosols in cloud.

$$t_{diff} \propto N_d^{-2/3}$$

Even though aerosol processing in clouds is not part of the PACE exercise, the availability of the ACE-2 data offers opportunity to also examine these processes in the validation experiment.

P8: GISS (A. Del Genio):

The boundary layer scheme is a second order closure scheme (Cheng et al. 2000), with sub-grid turbulence specified from the surface to the mid point of the first model layer. Cloud water is based on the prognostic scheme of Del Genio et al. (1996). Cloud cover is parameterised as a function of the relative humidity following Sundqvist et al. (1989).

The effect of aerosols on precipitation efficiency is taken into account via the auto-conversion process using three different parameterisations (Beheng, 1994; Berry, 1967 and Tripoli and Cotton, 1980). This is used to estimate the cloud lifetime effect on the AIE.

Cloud optical depth is parameterised using the same diagnosis of the droplet effective radius as in the Hadley model and equating volume radius to effective radius as $r_{eff} = 1.28\ r_v$. For a given optical depth and r_{eff}, cloud radiative properties are computed using the spectral dependence predicted by Mie theory (Hansen and Travis, 1974).

For sub-grid cloud parameterizations, cloud fraction is distributed evenly in all three dimensions in stable situations such that the cloud physical thickness is less than the GCM layer thickness. For unstable conditions the cloud is vertically developed and fractional cloudiness occurs only in the horizontal. Fractional cloudiness in time is used as a proxy for sub-grid scale spatial fractional cloudiness.

P9: PNNL (S. Ghan):

Cloud cover is crudely treated as zero for relative humidity less than 100% and 1 for relative humidity greater than 100%. Cloud optical depth is parameterised as in the Hadley Centre model. Auto-conversion of cloud water $R_{auto\text{-}w}$ and droplet number $R_{auto\text{-}N}$ are parameterised according to Ziegler (1985).

$$R_{auto-w} \propto q_c^{2.333} N_d^{-0.333}$$

$$R_{auto-N} \propto q_c^2$$

P7, Dalhousie Univ. (U. Lohmann):

Cloud cover is parameterised as a function of the relative humidity following Sundqvist et al. (1989).

Cloud albedo is parameterised following Rockel et al. (1991):

$$A = \frac{t}{(1-g)^{-1} + t}, \text{ where } t = W r_e^{-1.1}$$

r_e is dependent upon CDNC as indicated above.

The effect of aerosol on precipitation efficiency is expressed by the auto-conversion rate in the budget equations for the liquid water content $R_{auto\text{-}w}$.

$$R_{auto-w} \propto q_c^{4.7} N_d^{-3.3}$$, Beheng (1994)

The change in cloud droplet number concentration ($R_{auto\text{-}N}$) and self-collection of cloud droplets (R_{self}) are parameterised as:

$$R_{auto-N} = 7.7 10^{9} r R_{auto-w}$$

$$R_{self} = 1.29 10^{10} r_a \left(q_c / b \right)^2$$

where r_a is the air density, and b is the fractional cloud cover and

3.3.2.2 Correlation between effective radius and optical thickness

The observed differences in correlation between the optical thickness and the effective radius with remote sensing from ISCCP (Han et al. 1998) and GCM simulations (Lohmann et al. 2000-b and Menon et al. 1999) was discussed in this session. All results show, that for cases, where optical thickness is lower than *15*, the effective radius is positively correlated with *t* whereas for optical thickness > *15*, the correlation is negative and thus consistent with the indirect effect. Two hypotheses where tested with the ECHAM model (Lohmann et al., 2000-b), that could explain this phenomenon: (i) The ISCCP algorithms are based on vertically homogeneous clouds. Remotely sensed effective radius is representative of the upper cloud layer, which depends strongly on geometrical and thus also on optical thickness of the cloud layer for stratocumulus cloud types (explanation for the $t<15$ observations). The negative correlation for higher t can be a result of multi layer cloud systems. (ii) The change in sign of the correlation can be attributed to precipitating and non precipitating clouds. Based on ECHAM results grouped into precipitating and non-precipitation clouds, hypothesis (ii) could be confirmed (change in sign of correlation coefficient) whereas the grouping of single-layer and multi-layer clouds could not reproduce this change. However these results could be model specific and need to be further evaluated.

3.3.2.3 Closure Experiments: First Indirect Effect.

In situ measurements of the droplet concentration and the geometrical thickness have been analysed using data from vertical ascents and descents of the Merlin-IV aircraft during 8 flight missions. The analysis shows that the frequency distribution of the values of droplet mean volume as a function of altitude above cloud base, is contained within the limits of the adiabatic prediction for a concentration between 0.5 and 1.5 of the mean value, in agreement with the measured variability of the CDNC values, as discussed above. The data set also reveals that the difference between the effective diameter and the mean volume diameter in the upper half of the cloud thickness is smaller than 2µm, independently of the mean *CDNC* value (Pawlowska and Brenguier, 2000-a).

This closure study demonstrates that the adiabatic model of droplet growth is more realistic for radiative transfer calculations than the vertically uniform model. However, it also suggests that the droplet concentration varies significantly in a cloud layer, thus reflecting the variability of the vertical velocity at the CCN activation level. Additional variability results from the mixing processes and drizzle scavenging. The adiabatic model shall therefore be refined with consideration on the horizontal variability of *N* and the effects of sub-adiabaticity.

Based on in-situ observations, the radiative transfer calculations with a vertically uniform (VU-PPM) and an adiabatic stratified plan parallel (AS-PPM) cloud models were tested. The first step has been to identify a possible relationship between the effective diameter at the top of the AS-PPM, $r_{eAS}(H)$, and the value of effective radius to use in the VU-PPM, r_{eVU}, for the two models to produce the same values of reflected radiances in the visible (VIS) and near infra-red (NIR) domains. Simulations have been performed over a large range of cloud geometrical thickness *H* and droplet concentration *N*, and it has been demonstrated that there is no simple equivalence between the two models: $0.8 < d_{eVU} / d_{eAS}(H) < 1$, where the value of the ratio depends on both *H* and *N* (Brenguier et al. 2000-a). Further calculations of radiative transfer have thus been performed with the AS-PPM to provide (*H*,*N*) look-up tables of VIS and NIR radiances. A neural network technique has been developed for the retrieval of both *H* and *N* from measured radiances. The comparison with the values measured in situ constitutes the microphysics-radiation closure exercise in Cloudy-Column. The test confirms that the differences between a pure marine and a polluted case are clearly revealed by the VIS and NIR reflectances. However, the retrieved values of CDNC are systematically underestimated by the retrieval technique. This bias has been attributed to the horizontal heterogeneity of the cloud layer and the sub-adiabaticity of the microphysical field. These features are now considered for the development of a more realistic cloud model for radiative transfer calculations (Schüller et al., 2000).

3.3.2.4 Closure Experiments: Second Indirect Effect.

Drizzle measurements performed on board the Merlin-IV have also been analysed to identify possible differences between clean and polluted cases. Drizzle formation in a non precipitating cloud is mainly driven by the probability of production of a few big droplets. As for the cloud optical thickness, this probability is mainly determined by the cloud geometrical thickness, with the biggest droplets appearing at cloud top. It is thus crucial to clearly distinguish between the contribution of the cloud geometrical thickness and the contribution of CDNC to the onset of precipitation. The 8 analysed cases have been stratified according to their values of maximum geometrical thickness H_{max} and mean CDNC value N_{mean}, as described in Pawlowska and Brenguier (2000-a). For each case the maximum droplet mean volume diameter has been derived from its measured frequency distribution as the value at 97 % probability. A second estimate is derived from the adiabatic model as:

$$d_{v\max}^3 = \frac{C_w H_{\max}}{(p/6)\, r_w N_{mean}},$$

where C_w is the moist adiabatic condensation rate. These two characteristic values combine the effects of geometrical thickness and CDNC on the production of the biggest droplets. Plotted versus the maximum drizzle concentration measured in each case, they reveal that precipitation is formed only when the maximum droplet size is larger than 20 µm. The two marine cases with d_{vmax} of about 25 µm show significant drizzle production, while the three most polluted cases with d_{vmax} of about 15 µm show negligible precipitation. Three intermediate cases, with d_{vmax} of about 20 µm show intermediate values of drizzle concentrations. The scatter plots of maximum drizzle concentration versus the CDNC values normalized by N_{mean} demonstrate that only the most marine cases are significantly affected by drizzle scavenging, while the intermediate cases show detectable drizzle concentrations, but no effects on CDNC (Pawlowska and Brenguier, 2000-b).

3.4 Discussion and Recommendations

3.4.1 Physical Processes and Variables

3.4.1.1 Aerosol/Cloud Interaction (Responsible Person: J. Snider, with S. Guibert)

J.Snider summarized the suite of aerosol/CCN/CDNC closure studies. These results point to a disparity between the PDH aerosol data and two measurement systems on the Merlin-IV (UWYO CCN and FSSP-300). This disparity is most evident in closures attempted at low supersaturation (large dry size). This disparity is manifested as substantially larger concentrations derived from calculations based on the PDH aerosol data set, in comparisons with the measurements obtained from the Merlin. They also show that the disparity is larger for cases affected by continental pollution. Plausible explanations for the disparity are discussed below. Also presented are actions that are needed to test these hypotheses. This work shall be completed prior to the second PACE meeting in November 2000.

(i) Is it possible that a large fraction of the accumulation mode aerosol (i.e., as much as a 50% for the polluted cases) is not nucleating droplets? If true, this would imply that the accumulation mode particles exist as an external mixture of more-hygroscopic and less-hygroscopic particles. Since hygroscopicity (mixing state and growth factors) was measured at the PDH this hypothesis can be tested.

(ii) Is the version of Köhler theory that was applied here making the correct assumption with regard to the particle surface tension? The sensitivity of the results to this assumption needs to be tested.

(iii) Is the PDH aerosol data representative of that measured by the Merlin? This assumption needs to be tested in further detail using position data for the Merlin relative to the air parcel trajectories, using aerosol data from the UK C-130 and the CIRPAS Pelican, and using data from the PDH flybys that were performed by the Merlin.

(iv) How much variability is there in the measured PDH size spectra? To date we have expressed the PDH result as an average of the several DMA scans that were performed during each flight. Statistical variability in the PDH data should be examined. Further, PDH measurement uncertainties need to be addressed.

(v) Techniques used for the evaluation of N_{mean} from the Fast-FSSP need to be extended to cases without aircraft ascents and descents, modulo some modifications of the procedure.

3.4.1.2 Cloud/Radiation Interaction (Responsible Person: L. Schüller)

The latest results presented by L. Schüller demonstrate that the retrieval technique based on the adiabatic model and the radiance measurements is able to distinguish between clean and polluted cases, though the retrieved value of N_{mean} are twice as small as the one measured in situ. The retrieved frequency distributions of N_{mean} versus H_{max} reveals that the bias is not due to noise in the measurements but rather that the information is available in the data, though it is not interpreted correctly by the retrieval technique. Next steps to improve the method will be to assume more realistic droplet size distributions in the model and to take into account the spatial heterogeneity of the microphysical fields. Improvements will be reported at the next PACE meeting.

3.4.1.3 Precipitation Efficiency (Responsible Person: H. Pawlowska)

The results presented by H. Pawlowska provide an accurate estimation of the droplet diameter threshold for the auto-conversion process. However, in order to be directly comparable with the values used in the parameterisations, it will be better to characterise the max droplet sizes by the largest droplets of the size distribution instead of its mean volume diameter. This improvement will be accomplished by July 2000 and the partners will be informed upon the new threshold value.

3.4.1.4 Turbulent Mixing at the Cloud Top (Responsible Person: S. Malinowski)

The EULAG LES model (Grabowski and Smolarkiewicz 1996, Smolarkiewicz and Margolin 1997) running at IGUW will be used to simulate mixing processes at the top of the cloud layer and validated versus measurements of the droplet distributions at the micro-scale. They will be used to quantify the effects of mixing in term of turbulent fluxes between the BL and the free troposphere.

3.4.2 Selection of the Case Studies (Responsible Person: J. L. Brenguier)

After discussion on the available data for each case, June 26 has been selected for the clean case and July 9 for the polluted case. The series of flights from July 16 to 19 have also been considered as a very interesting case of pollution event with a significant time evolution over the 4 days. However, their analysis is more complex and it has been decided to postpone their analysis after validation of the two most simple cases selected above. Partner 1 is in charge (Sept. 2000) of completing the Table that summarizes the whole experiment, with additional information upon data from the UK-C130, the CIRPAS Pelican and any data set that could be useful for the project.

3.4.3 Initialisation Data Set for the SCMs

The data set must be ready by September first 2000 for the modellers to start the exercise and report on preliminary results at the next PACE meeting in November 2000. J. Feichter (P5) will host the data base in the Max Planck Inst. Computer system.

3.4.3.1 Dynamical and Thermodynamical Fields (Responsible Person: J. Feichter)

J. Feichter will provide the data base with an initialisation data set based on the ECMWF and ECHAM4 fields, for the period June 15 to July 22, 1997:

ECMWF
- Operational Analysis (T213)
- surface fields
- 31 level model level data
- pressure level data
- Different forecast products (e.g. first guess)
- Several types of observations (as e.g. radiosondes, SYNOP, SHIP, ...)

ECHAM4 T106 (nudged with the ECMWF operational analysis):
- model output (surface as well as level data)

3.4.3.2 Aerosol Data Set (Responsible Person: J. Snider & S. Guibert)

Attempts aimed at closing the link between observed CDNC (selected based on the tests for adiabaticity and the absence of drizzle) and predictions based on both Köhler and parcel models, initialised with the aerosol data from PDH, are not yet satisfactory. The CDNC values based on the PDH data set are substantially larger than those observed. It has been concluded that the most likely origin for the observed bias is measurement error associated with the PDH size distribution, particularly for the accumulation mode sizes (dry diameter > 0.1 um),

or associated with the PDH measurements of aerosol composition. It was decided to test three data sets for initialisation of the SCMs.

(i) The PDH Data Set as it is reported in the ACE-2 data base.

(ii) The Reverse CCN Data Set. This refers to a virtual aerosol distribution that produces, via the Köhler theory, CCN spectra comparable to the measured ones, by assuming all aerosol particles are sulphate.

(iii) The Modified PDH data Set. As some aerosol properties were not directly measured at PDH, but rather inferred from indirect measurements, there are possibilities to modify the PDH data set in such a way that the closure experiment with the Köhler and the parcel models is improved. Various hypotheses will be tested, i.e. (i) to (iv) in Sec. 3.4.1.1, for producing what is referred to as the modified PDH data set for testing the GCM parameterisations.

3.4.3.3 Surface Turbulent Fluxes (Responsible Person: F. Troude)

Vertical profiles of the turbulent fluxes, from the surface to the top of the BL, will be derived from aircraft measurements made with the Merlin-IV, the UK C130 and the CIRPAS Pelican.

3.4.3.4 Satellite images from H-24 to H-0 (Responsible Persons: L. Schüller & G. Tselioudis)

Meteosat images (VIS and IR) will be extracted from the archive for the two selected case studies from 24 hours before the flight and provided to the data base (L. Schüller). G. Tselioudis (GISS) will provide similar images from the ISCCP data set.

3.4.4 Validation Data Set for the SCMs

3.4.4.1 CDNC (Responsible Person: H. Pawlowska)

The present statistics on CDNC will be extended for the two selected case studies by including clear air samples in the first class, but still for samples made at an altitude between $0.4\ H_{max}$ and $0.6\ H_{max}$, with and without condition on drizzle concentration. An alternative procedure will be defined for flights where ascents and descents are not available, such as the inter-calibration flights that are used for the aerosol/CDNC interaction, in order to characterize their CDNC typical value.

3.4.4.2 LWC and LWP (Responsible Person: H. Pawlowska, M. Schröder, F. Troude)

Statistics of LWC and LWP will be derived from the measurements for the two selected case studies.

The statistics of LWC will be stratified over five levels of altitude above cloud base. Frequency distributions will be produced for the absolute values and the values normalised by the adiabatic LWC at the corresponding altitude level (H. Pawlowska).

Statistics of liquid water path (LWP) will be derived from the above stratified LWC distributions, by assuming random overlap and the most coherent overlap of the LWC values. The bias between the two distributions will be quantified and mean values over the grid box will be calculated (H. Pawlowska).

A second LWP frequency distribution will be derived from the CASI measurements of cloud radiances (M. Schröder).

Finally, a third LWP frequency distribution will be calculated from the simulations made with the Meso-NH LES model after its validation with the in situ measured horizontal statistics of LWC and the measured statistics of radiances from CASI (F. Troude).

3.4.4.3 Drizzle Concentration (Responsible Person: H. Pawlowska)

Statistics of drizzle particles will be provided in term of number concentration and drizzle water content. The frequency distributions will be calculated over cloud samples defined as samples with $N_d > 5\ cm^{-3}$.

3.4.4.4 Cloud Layer Base and Top (Responsible Person: H. Pawlowska)

The mean cloud base altitude and mean cloud depth will be derived from the series of ascents and descents.

3.4.4.5 Vertical Velocity at Cloud Base (Responsible Person: S. Guibert)

Frequency distributions of vertical velocity will be calculated at two levels: below cloud base and within the cloud layer.

3.4.4.6 Multi-spectral Radiances, cloud fraction and Cloud Albedo (Responsible Person: L. Schüller)

The cloud fraction will be derived from CASI images. Spectrally integrated short wave albedo will be calculated from the OVID measurements in the spectral range between 0.6 and 1.6 µm. Extended range albedo will be derived with the MOMO radiative transfer model over the spectral range between 0.25 and 4 µm. Similar data will be provided over the spectral bands that are used in the radiation modules of the participating GCM's.

4. General discussion on future requirements for satellite measurements

On the side of the PACE meeting, a short session of one hour on Friday morning has been dedicated to a general discussion on the satellite measurements that are required for improving the experimental assessment of the aerosol indirect effect. After an introduction by J. Hansen, head of the Goddard Institute, regarding a proposed new initiative to assess aerosol climate forcing, M. Mishchenko (GISS) made a review of the physical parameters that are relevant to the indirect effect and of the required accuracy in the retrieval of these parameters from satellite measurements. The PACE group has suggested some improvements to these requirements.

5. Conclusions

The outcomes of the first PACE meeting are the following:
- Information have been exchanged between experimentalists and modellers, for the modellers to evaluate precisely the type of data that are available to validate the parameterisations, their accuracy and the present limitations of the closure exercises, and for the experimentalists to understand how the data should be processed and interpreted in order to facilitate the validation exercise.
- General discussions have been conducted between the two communities in order to clarify concepts and the physical representations of the variables used in the models.
-Decisions have been taken for extending the data processing and interpretation towards directions needed by the modellers to validate their parameterisations. Two case studies have been selected. The data base will be hosted by Partner 5 and the contributions from the experimentalists will be provided before Sept. 2000 for the modellers to start SCM simulations, which will be discussed at the next PACE meeting. The second PACE meeting will be hosted by the Freie Univ. of Berlin (Partner 2), from 6 to 10 November 2000.

6. References

Abdul-Razzac, H., and S. J. Ghan, 2000: A parameterization of aerosol activation. 2. Multiple aerosol types. *J. Geophys. Res*., **105**, 6837-6844.

Beheng, K.D., 1994. A parameterization of warm cloud microphysical conversion processes. *Atmos. Res*., **33,** 193-206.

Berry, E.X., 1967: Cloud droplet growth by collection. *J. Atmos. Sci*., **24**, 688-701.

Borys R.D., D.H. Lowenthal, M.A. Wetzel, F. Herrera, A. Gonzalez and J.. Harris, 1998: Chemical and microphysical properties of marine stratiform cloud in the North Atlantic. *J. Geophys. Res.*, **103**, 22073-22085.

Brenguier, J. L., H. Pawlowska, L. Schüller, R. Preusker, J. Fischer, and Y. Fouquart, 2000-a: Radiative properties of boundary layer clouds: droplet effective radius versus number concentration. *J. Atmos. Sci*. 57, 803-821.

Brenguier, J. L., P. Y. Chuang, Y. Fouquart, D. W. Johnson, F. Parol, H. Pawlowska, J. Pelon, L. Schüller, F. Schröder and J. R. Snider, 2000-b; An overview of the ACE-2 CLOUDYCOLUMN Closure Experiment. *Tellus.* **52B**, 814-826.

Chuang, C. C. and J. E. Penner, 1995: Effects of anthropogenic sulphate on cloud drop nucleation and optical properties. *Tellus **47B,*** 566-577.

Cheng,Y., V.M. Canuto and A.M. Howard, 2000: A second-order closure turbulence model in the PBL. *J. Atmos. Sci*., (submitted).

Del Genio, A.D., M.-S. Yao and K. K.-W. Lo, 1996: A prognostic cloud water parameterization for global climate models. *J. Climate*, **9,** 270-304.

Edwards, J. M., and A. Slingo, 1996: Studies with a flexible new radiation code. I: choosing a configuration for a large-scale model. *Quart. J. Roy. Meteor. Soc*., **122**, 689-719.

Ghan, S.J., L.R. Leung, R.C. Easter, and H. Abdul-Razzak, 1997: Prediction of droplet number in a general circulation model. *J. Geophys. Res*., **102,** 21,777-21,794.

Grabowski, W. G. and P. K. Smolarkiewicz, 1996: Two-time level semi-Lagrangian modelling of precipitating clouds. *Mon. Wea. Rev.,* **124,** 487-497.

Guibert, S., J. Snider, and J.-L. Brenguier, 2000: A Closure experiment on the CCN activation process in ACE-2 Cloudy-Column. *Preprints of the 13th Int. Conf. on Clouds and Precip*, Reno, USA.

Gultepe, I. and G.A. Isaac, 1999: Scale effects on averaging of cloud droplet and aerosol number concentrations: Observations and models. *J. Clim.*, **12**, 1268-1279.

Han, Q., W. B. Rossow, J. Chou, and R. M. Welch, 1998: Global survey of the relationships of cloud albedo and liquid water path with droplet size using ISCCP. *J. Climate*, **11,** 1516-1528.

Hansen, J.E. and L.D. Travis, 1974: Light scattering in planetary atmospheres. *Space. Sci. Rev.,* **16,** 527-610.

Khairoutdinov, M. and Y.Kogan, 2000: A New Cloud Physics Parameterization in a Large-Eddy Simulation Model of Marine Stratocumulus. *Monthly Weather Review*, **128**, 229-243.

Leaitch, W. R., G. A. Isaac, J. W. Strapp, C. M. banic and H. A. Wiebe, 1992: The relationship between cloud droplet number concentrations and anthropogenic pollution: Observations and climatic implications. *J. Geophys. Res.*, **97,** 2463-2474.

Lin, H., and W. R. Leaitch, 1997: Development of an in-cloud aerosol activation parameterization for climate modelling. *Preprints of the WMO workshop on cloud microphysics* . Mexico

Liu P. S. K., W. R. Leaitch, C. M. Banic, S. M. Li, D. Ngo and W. J. Megaw, 1996: Aerosol observations at Chebogue Point during the 1993 North Atlantic Regional Experiment: Relationships among cloud condensation nuclei, size distribution, and chemistry, *J. Geophys. Res.*, **101**, 28971-28990.

Lohmann, U., J. Feichter, C.C. Chuang and J.E. Penner, 1999: Predicting the number of cloud droplets in the ECHAM GCM. *J. Geophys. Res*. **104,** 9169-9198

Lohmann, U., J. Feichter, J. E. Penner, and W. R. Leaitch, 2000-a: Indirect effect of sulfate and carbonaceous aerosols: A mechanistic treatment, *J. Geophys. Res.*, in press.

Lohmann,U., G. Tselioudis, and C. Tyler, 2000-b: Why is the cloud albedo particle size relationship different in optically thick and optically thin clouds. *Geophys. Res. Lett.,* **27,** 1099-1102.

Martin, G. M., D. W. Johnson and A. Spice, 1994: The measurement and parameterization of effective radius of droplets in warm stratocumulus clouds. *J. Atmos. Sci*., **51**, 1823-1842.

Menon, S, A. D. Del Genio, D. Koch, and G. Tselioudis, 1999: An estimate of the aerosol indirect effect using a coupled chemistry-climate model and comparison with satellite data, *EOS (AGU Trans.)*, AGU Fall Meeting, San Francisco, CA.

Pawlowska, H. , and J. L. Brenguier, 2000-a: Microphysical properties of stratocumulus clouds during ACE-2. *Tellus.,* **52B**, 867-886.

Pawlowska, H., and J.-L. Brenguier, 2000-b: The indirect effect of aerosols on climate: Effect of aerosol properties on precipitation efficiency. *Preprints of the 13th Int. Conf. on Clouds and Precip*, Reno, USA.

Putaud, J. P., R. Van Dingenen, M. Mangoni, A. Virkkula, H. Maring, J. M. Prospero, E. Swietlicki, O. H. Berg, R. Hillamo , and T. Mäkelä , 2000: Chemical mass closure and assessment of the origin of the submicron aerosol in the marine boundary layer and the free troposphere at Tenerife during ACE-2. *Tellus.* **52B,** 141-168.

Rockel, B., E. Raschke and B. Weyres, 1991: A Parameterization of Broad Band Radiative Transfer Properties of Water, Ice and Mixed Clouds. *Beitr. Phys. Atmos.* **64,** 1-12.

Schüller, L., J. L. Brenguier, and H. Pawlowska, 2000: The indirect effect of aerosols on climate: Observations with an airborne radiometer. *Preprints of the 13th Int. Conf. on Clouds and Precip*, Reno, USA.

Slingo, A., 1989: A GCM Parameterization for the Shortwave Radiative Properties of Water Clouds. *J. Atmos. Sci*., **46,** 1419-1427.

Smolarkiewicz, P. K. and L. G. Margolin, 1997: On forward-in-time differencing for fluids. An Eulerian / semi-Lagrangian non-hydrostatic model for stratified flows. *Atmos.-Ocean,* **35,** 127-152.

Snider, J. R., and J. L. Brenguier, 2000: A comparison of cloud condensation nuclei and cloud droplet measurements obtained during ACE-2. *Tellus.,* **52B,** 827-841.

Sundqvist, H., E. Berge and J.E. Kristjansson, 1989: Condensation and cloud parameterization studies with a mesoscale numerical weather prediction model. *Mon. Wea. Rev.,* **117,** 1641-1657.

Tripoli, G.J. and W.R. Cotton, 1980: A numerical investigation of several factors contributing to the observed variable intensity of deep convection over South Florida. *J. Appl. Meteor.,* **19**, 1037-1063.

Wilson, D. R. and Ballard, S. P., 1999. A microphysically based precipitation scheme for the Meteorological Office Unified Model. *Quart. J. Roy. Meteor. Soc.*, **125**, 1607-1636.

Ziegler, C.L., 1985: Retrieval of thermal microphysical variables in observed convective storms, 1, Model development and preliminary testing. *J. Atmos. Sci.*, **42**, 1487-1509.

AGENDA FOR THE PACE WORKSHOP
AT NASA GISS, NEW YORK:
May 1 to May 5, 2000

Monday,May 1 and Tuesday, May 2:
Preparatory meeting with experimentalists and S. Menon.

Wednesday, May 3: Aerosol/cloud interaction
Morning:
09:00 - 9:10: Welcome speech by Surabi Menon
09:10- 09:30: Introduction by Jean-Louis Brenguier

Presentation by modelers on their parameterisation schemes

09:30- 10:00: Hadley Centre - Andy Jones
10:00-10:30: GISS - Surabi Menon

10:30-10:50: Coffee Break

10:50-11:20: PNLL - Steve Ghan
11:20-12:00: MPI- Johann Feichter
12:00-12:30: Discussion

12:30-14:00: Lunch Break

Afternoon:
14:00-14:30: General Description of ACE-2 by Jean-Louis Brenguier
14:30-15:00: Methodology for the experimental characterization of CDNC and cloud geometrical thickness by Hanna Pawlowska

15:00-15:30: Coffee break

15:30-16:00: Results of the aerosol/CDNC closure experiment in ACE-2 by Sarah Guibert
16:00-16:30: Results of the CCN/CDNC closure experiment in ACE-2 by Jefferson Snider

16:30-17:00: Discussion

17:00: Reception at GISS

Thursday, May 4: Cloud/Radiation interaction and sub-grid parameterisations

Morning:
Presentation by modelers on their parameterisation schemes

09:00-09:30: Hadley Centre - Dave Roberts
09:30-10:00: GISS - Tony Del Genio

10:00-10:20- Coffee break

10:20-10:50: PNLL - Steve Ghan
10:50-11:30: MPI- Ulrike Lohmann and Johann Feichter
11:30-12:30: Discussion

12:30-14:00: Lunch Break

Afternoon:
Results of the cloud and radiation closure experiment in ACE-2.
14:00-15:00: Hanna Pawlowska: cloud properties
15:00-15:45: Lothar Schüller: radiative properties

15:45-16:00: Coffee break

16:00-16:30: Results of the experimental study on precipitation efficiency.
16:30-17:00: LES Modelling with the IGUW LES model
17:00-17-30: LES Modelling with the Meso-NH model

Friday, May 5: General Discussion
Morning:
09:00-10:00: General discussion on future requirements for satellite measurements

10:00-11:00: Selection of the case studies and initialisation data sets.

11:00: 11:20: Coffee Break

11:20-12:30: Actions for the aerosol/cloud microphysics validation tests

12:30-14:00: Lunch Break

Afternoon:
14:00-16:30: Actions for validation tests of the parameterisations for the cloud fraction sub-grid and radiative transfer parameterisation schemes

16:30 Closing of the Meeting.